

LISA Far Field Phase Patterns

Eugene Waluschka

NASA/Goddard Space Flight Center/551.0

Greenbelt, Maryland 20771

1. INTRODUCTION

The Laser Interferometer Space Antenna¹ (LISA) consists of three spacecraft in orbit about the sun. The orbits are chosen such that the three spacecraft are always at (roughly) the vertices of an equilateral triangle with 5 million kilometer leg lengths. Even though the distances between the three spacecraft are 5 million kilometers, the expected phase shifts between any two beams, due to a gravitational wave, only correspond to a distance change of about 10 pico meters, which is about 10^{-5} waves for a laser wavelength of 1064 nm.

To obtain the best signal-to-noise ratio, noise sources such as changes in the apparent distances due to pointing jitter must be controlled carefully. This is the main reason for determining the far-field phase patterns of a LISA type telescope. Because of torque on the LISA spacecraft and other disturbances, continuous adjustments to the pointing of the telescopes are required. These pointing adjustments will be a "jitter" source. If the transmitted wave is perfectly spherical then rotations (jitter) about its geometric center will not produce any effect at the receiving spacecraft. However, if the outgoing wave is not perfectly spherical, then pointing jitter will produce a phase variation at the receiving spacecraft.

The following sections describe the "brute force" computational approach used to determine the scalar wave front as a function of exit pupil (Zernike) aberrations and to show the results (mostly graphically) of the computations. This approach is straightforward and produces believable phase variations to sub-pico meter accuracy over distances on the order of 5 million kilometers. As such this analyzes the far field phase sensitivity to exit pupil aberrations.

2. DIFFRACTION INTEGRAL

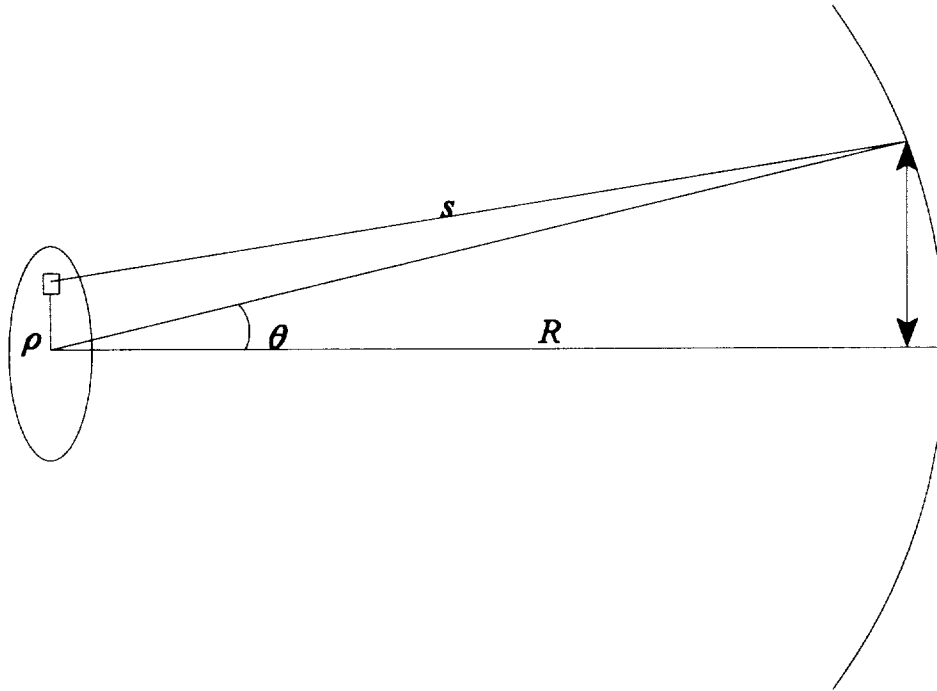
The (scalar) far field is described by²

$$A(X,Y,Z) \cdot e^{i\frac{2\pi}{\lambda}R} \cdot e^{i\frac{2\pi}{\lambda}\phi(X,Y,Z)} = \iint E(x,y,z) \frac{e^{i\frac{2\pi}{\lambda}(Z_n + S)}}{S} dx dy$$

where (X,Y,Z) are the far field variables that lie on a sphere of radius, R , of 5 million kilometers and centered on the center of the exit pupil as shown in the figure below. The integration is over the exit pupil and Z_n is the exit pupil aberration. The quantity of interest is ϕ , the deviation of the phase from a spherical wave. Determining ϕ is not a new quest. Nijboer's 1947³ paper derives a formula for ϕ in terms of Bessel functions for given aberrations. However the problem with just using the formula is that complex variations in the amplitude and phase are difficult to handle. A straightforward numerical integration of the above integral is easy to implement and creates a general purpose capability that can handle central obscurations and "spiders" and non-uniform pupil functions $E(x,y,z)$. It should be noted that the speed of today's computers makes this approach very attractive.

The numerical approximation of the diffraction integral, in this case, requires the addition of very large numbers, s , measured in millions of kilometers and very small numbers, Z_n , measured in fractions of a wavelength. This mismatch

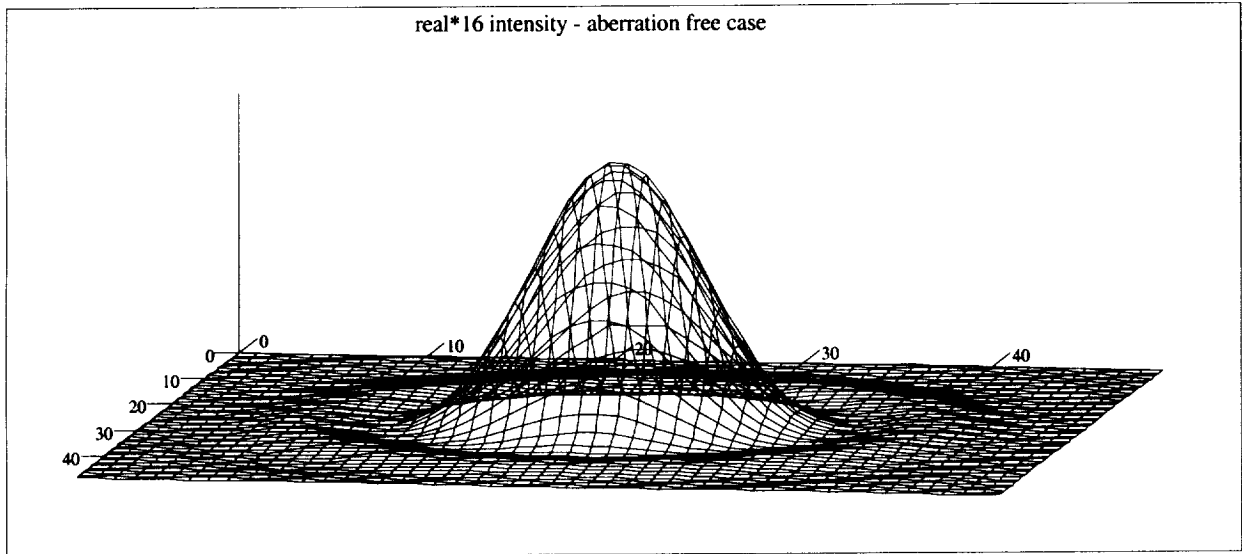
cannot be handled by "double precision" (eight byte) computer arithmetic. However, an easy solution is to simply use quadruple precision (16 byte) available on Digital Alpha computers and supported by their FORTRAN compilers. This "quad" precision distinguishes between 5 million kilometers and 5 million kilometers plus one pico meter, easily. With quad precision the "machine epsilon" is about $9.6 \cdot 10^{-35}$



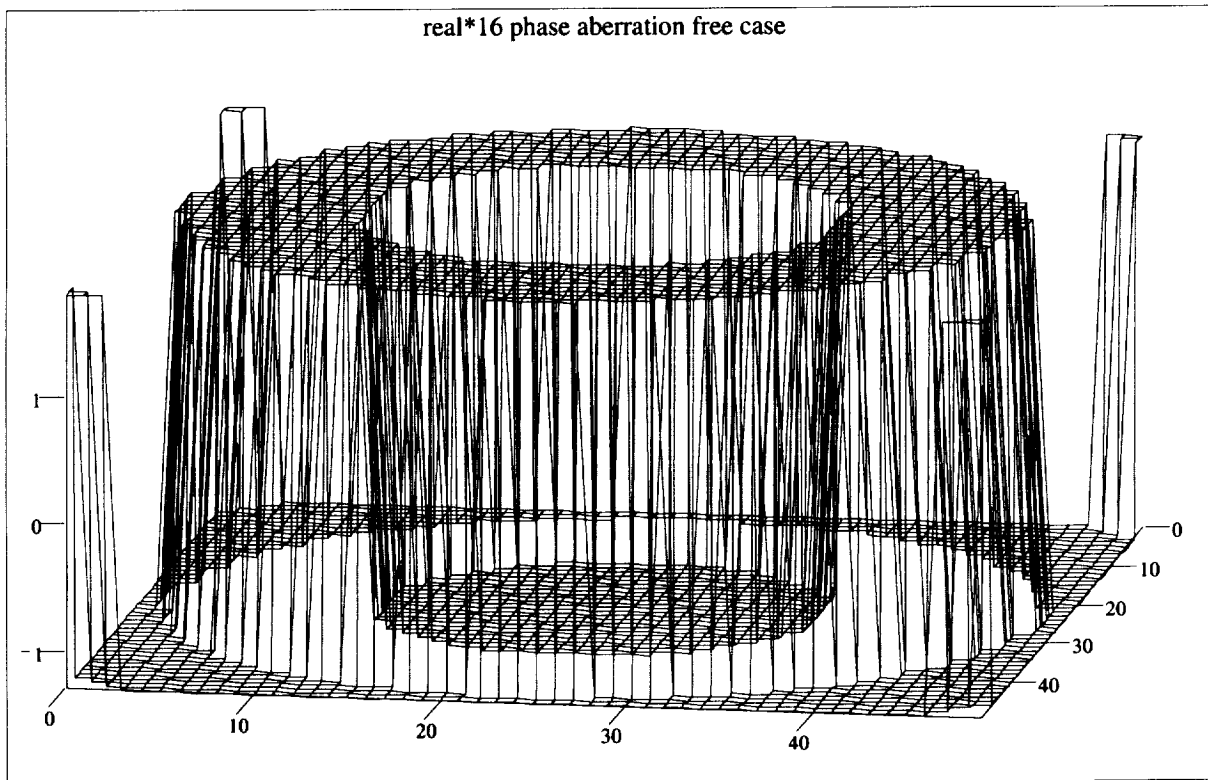
Exit pupil and far field sphere

3. NO ABERRATIONS

As a check on the numerical integration procedure, the next two plots show the far field intensity and phase out to the second dark ring for the case of an aberration-free uniformly illuminated unobstructed 30 cm exit pupil. As can be seen, the intensity, on the 5 million kilometer sphere, is the Airy diffraction pattern and the phase, in radians, shows the appropriate, π , discontinuity at the zero intensity points.



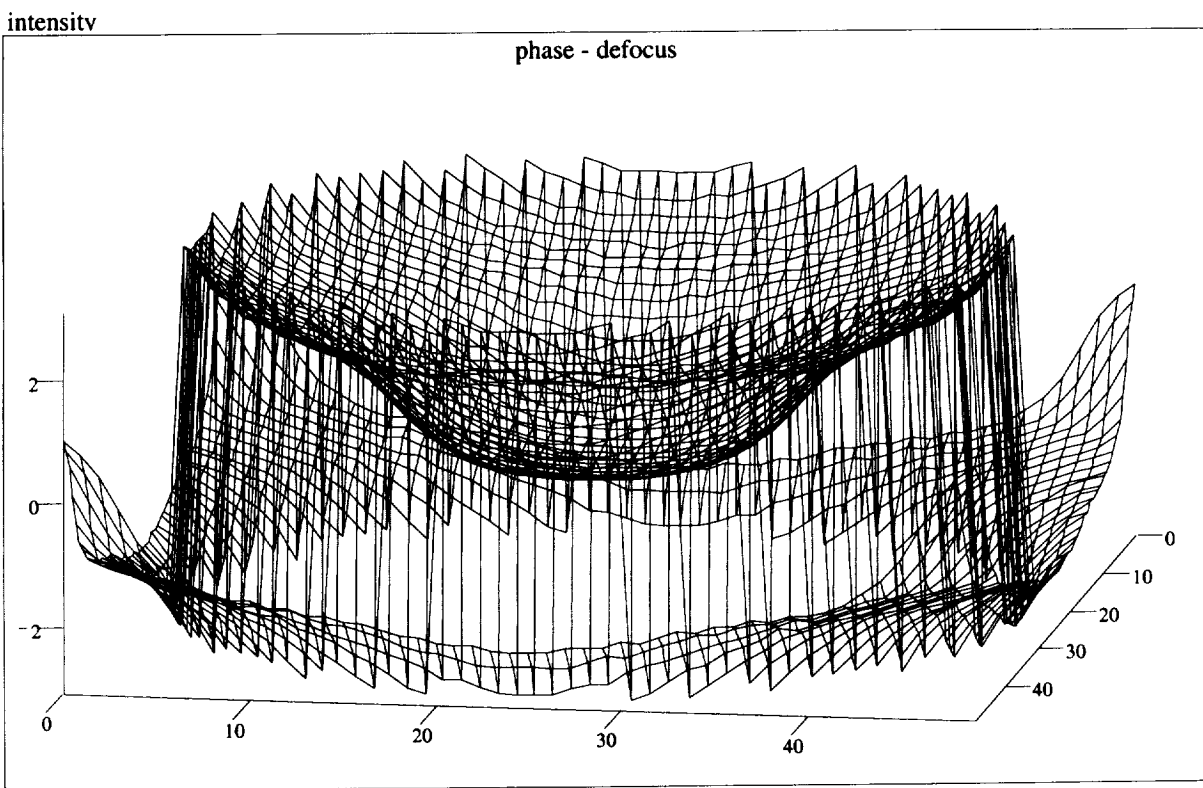
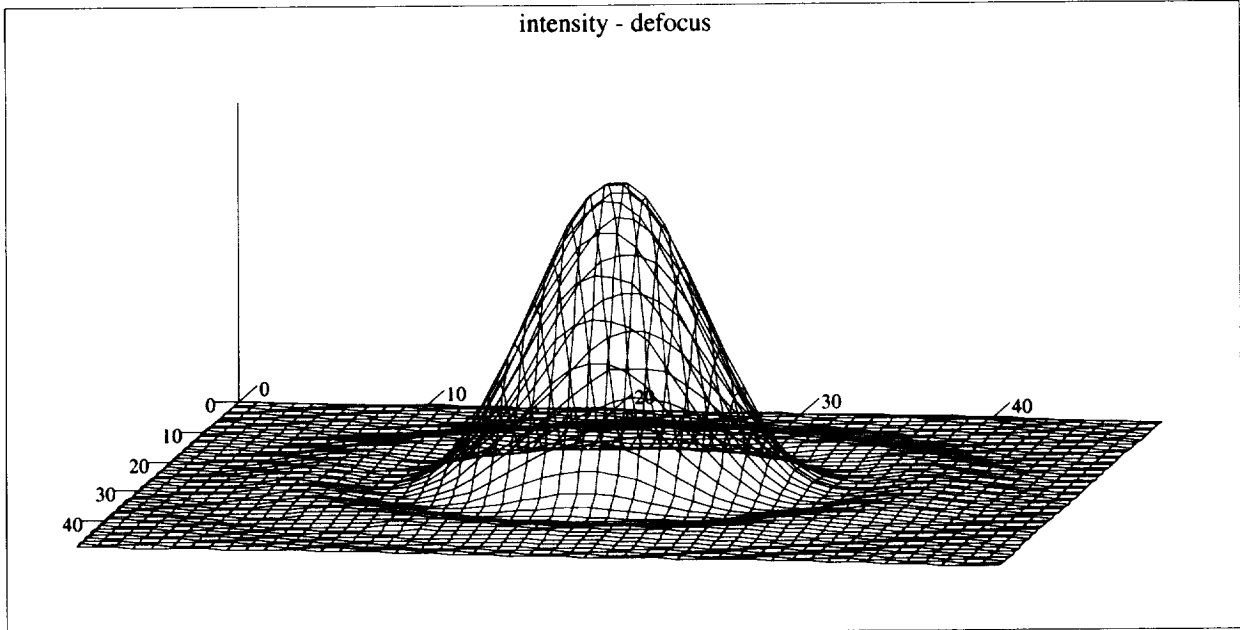
intensity



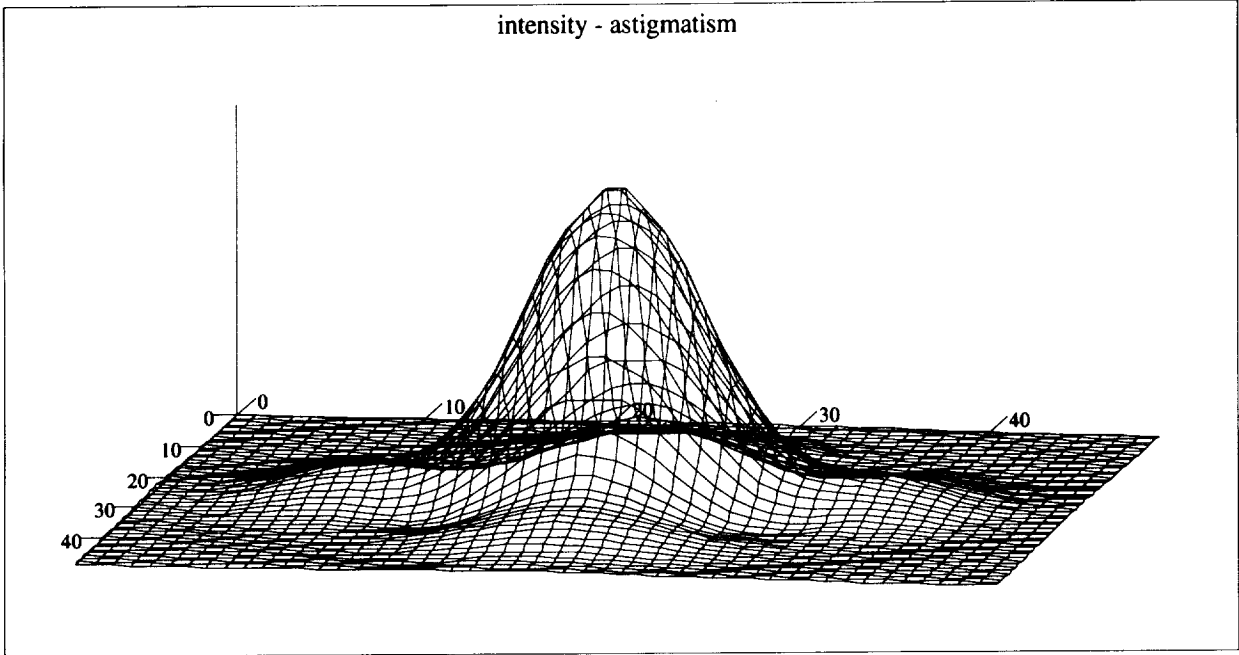
phase

4. DEFOCUS AND ASTIGMATISM

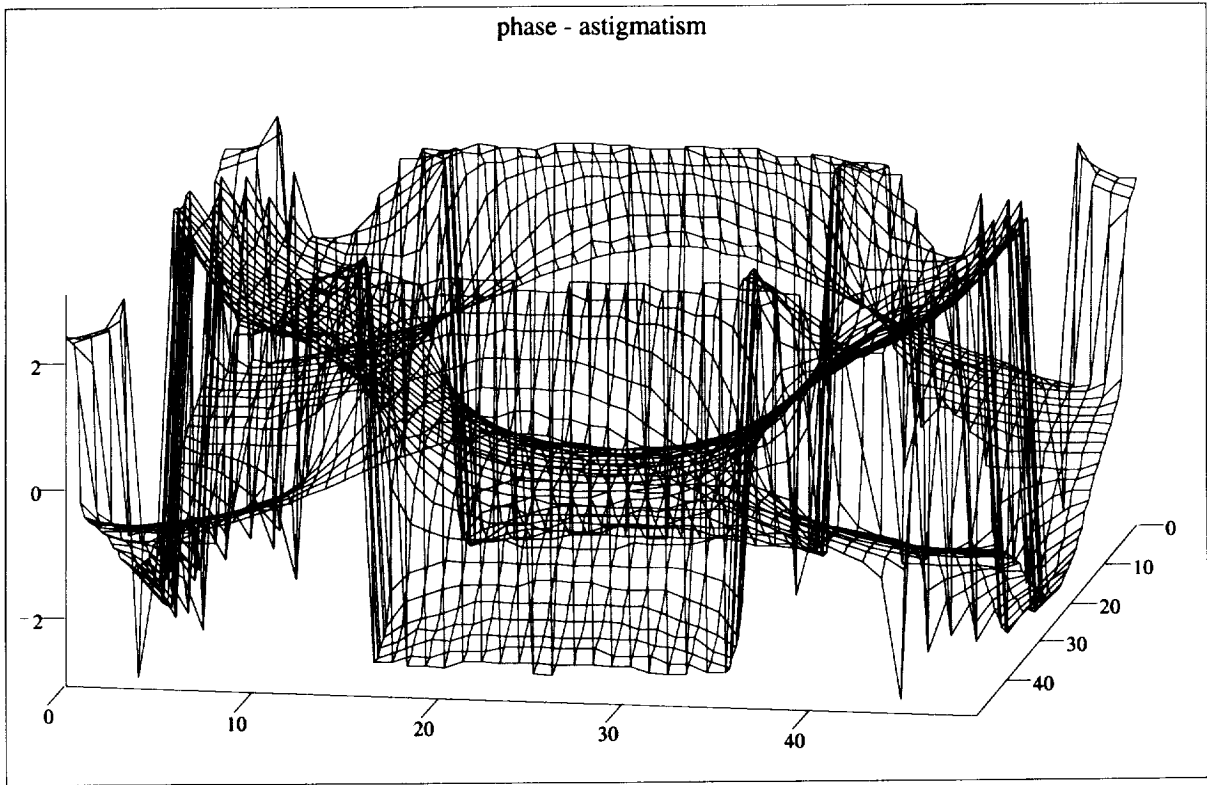
If we introduce a $1/10 \lambda$ rms wave front aberration in the exit pupil and perform exactly the same numerical integration, we get the following results for the intensity and phase distributions on the 5 million kilometer sphere.



phase



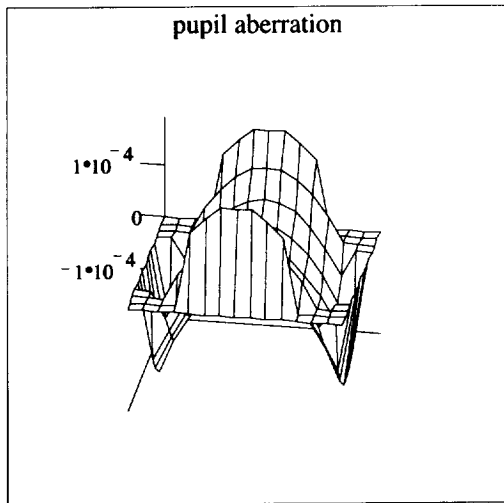
intensity



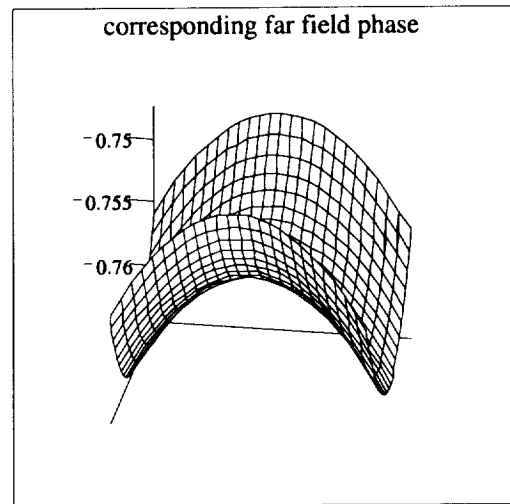
phase

5. REDUCED FIELD OF VIEW

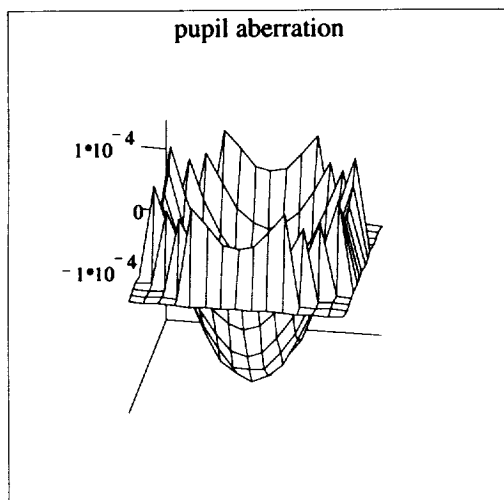
The field of view in the above plots is out to the second Airy dark ring. The above plots are presented primarily to show the reader the "large" scale phase variations. However, in order to maximize the signal and avoid phase discontinuities the central portion, out to the 95% of peak intensity, points are of particular interest. The first dark ring subtends an angle of $4.3 \cdot 10^{-6}$ radians and the 95% points subtend an angle of $0.53 \cdot 10^{-6}$ radians. The plots below show only the behavior of the phase, on the 5 million kilometer sphere, within this smaller field of view. The spatial extent is from -2.64 to +2.64 kilometers for both x and y, and the vertical axis is the phase in radians. The pupil aberrations are $1/10 \lambda$ rms of the indicated Zernike functions for Z4 to Z15 (in the CODE-V™ numbering scheme). Both the pupil aberration and the far-field phase distribution are shown to emphasize the similarities.



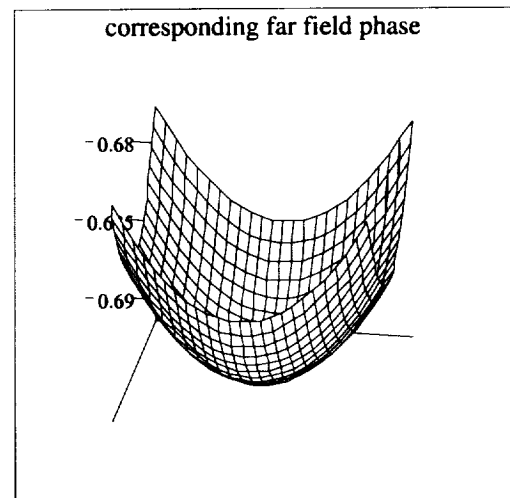
z4



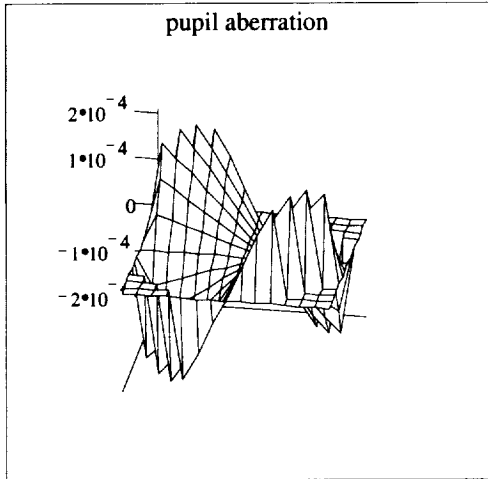
p4



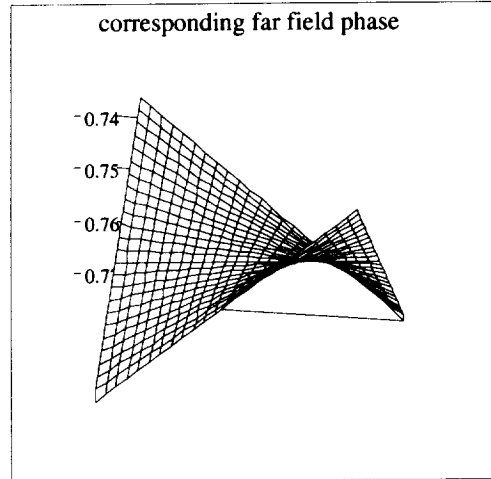
z5



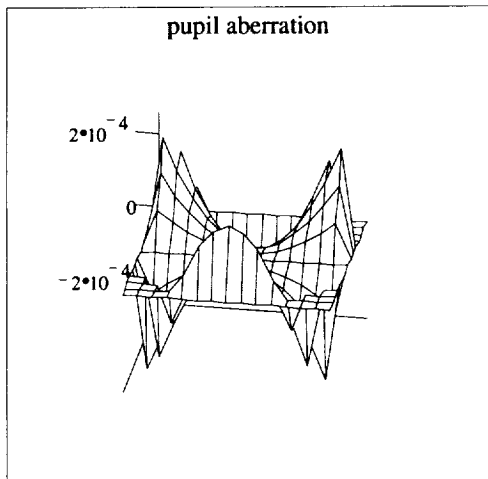
p5



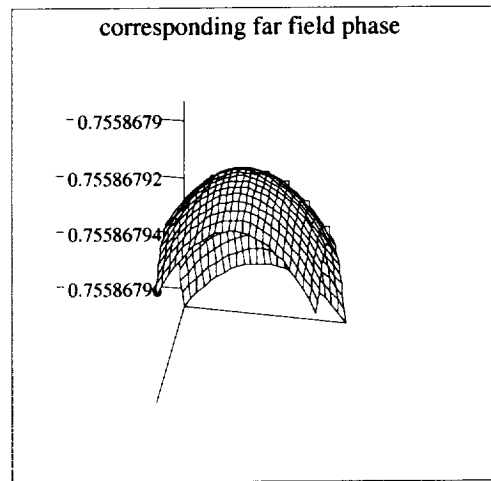
z6



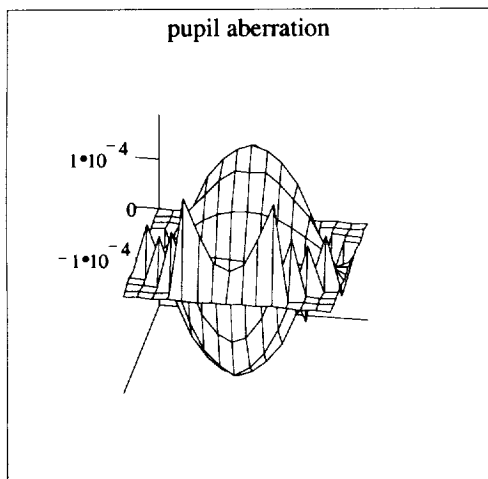
p6



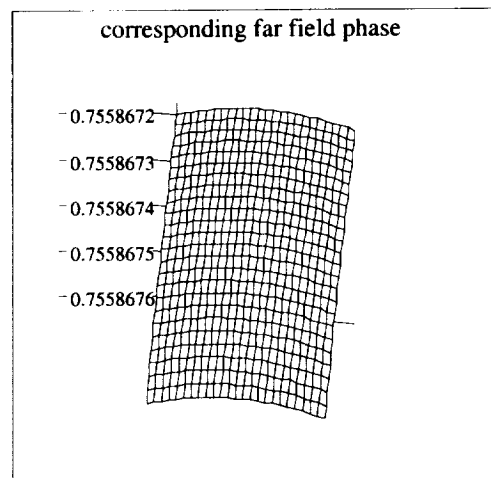
z7



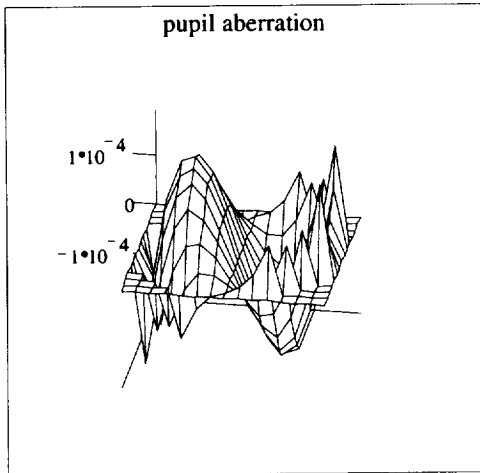
p7



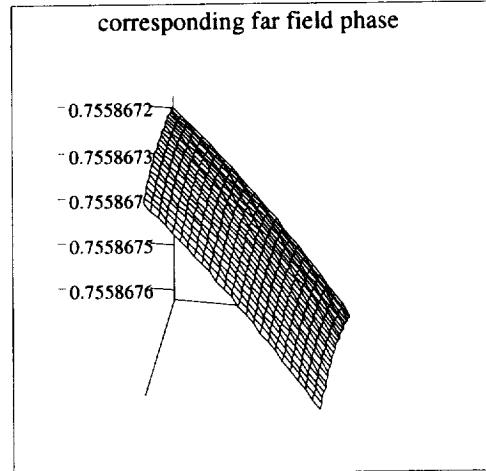
z8



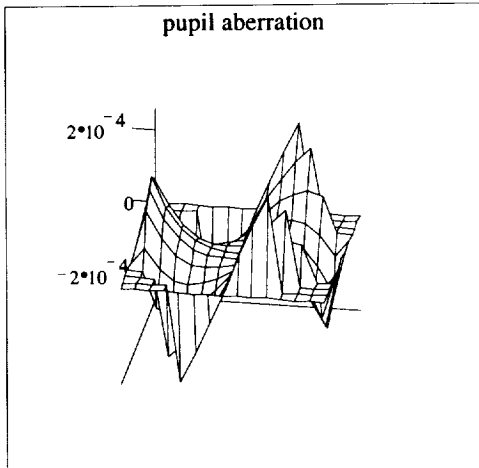
p8



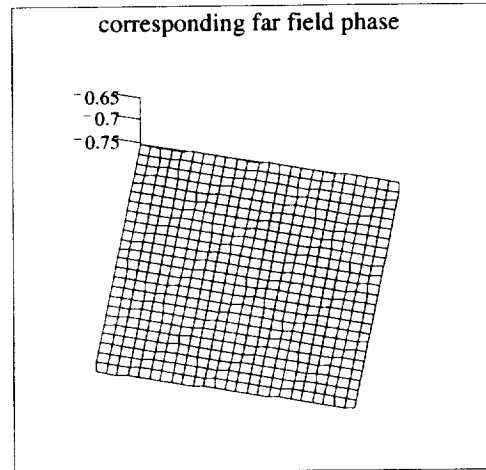
z9



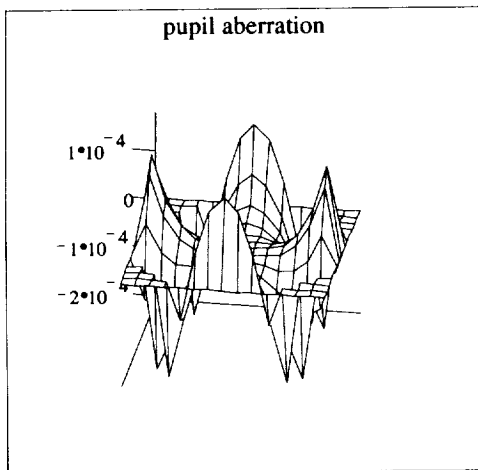
p9



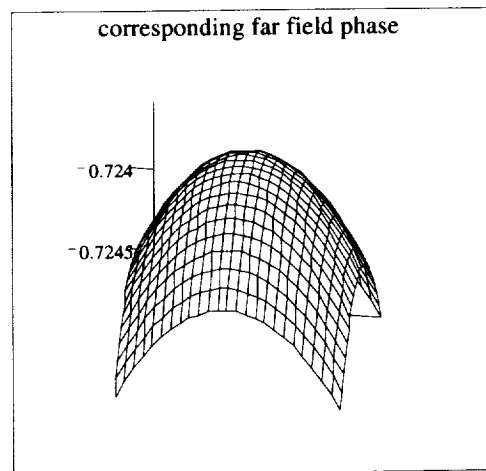
z10



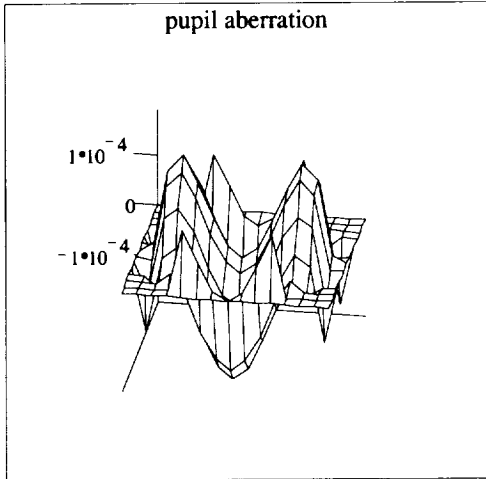
p10



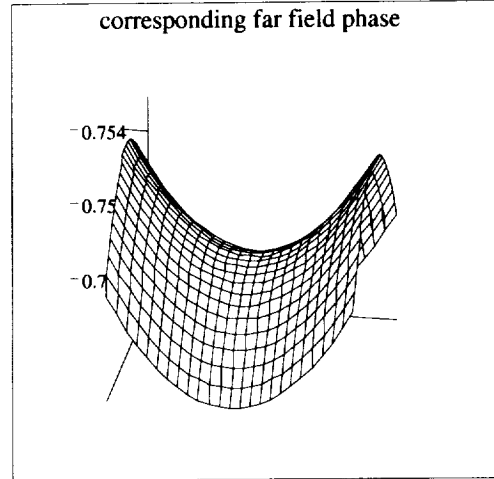
z11



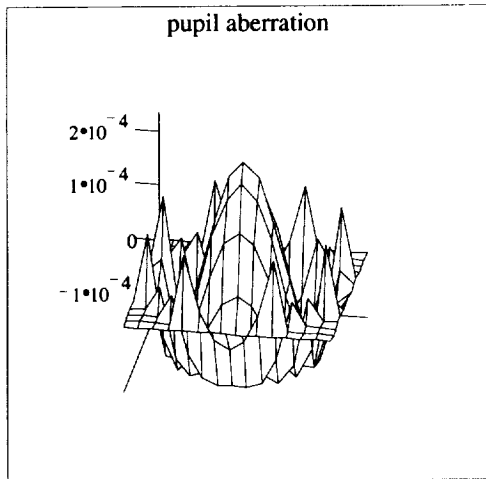
p11



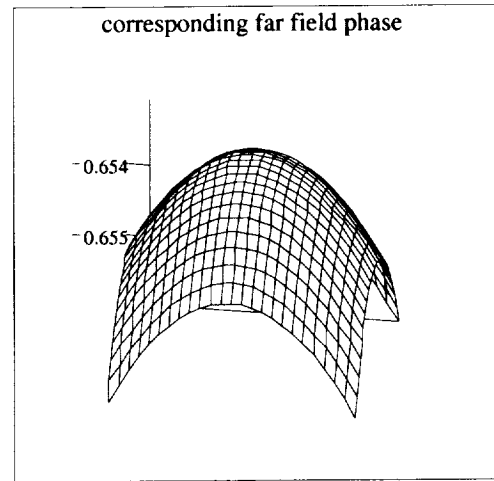
z12



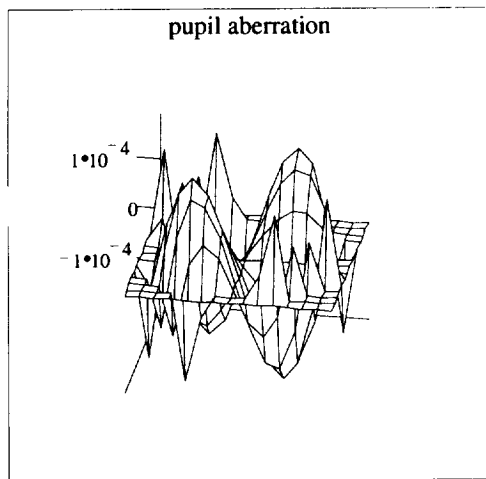
p12



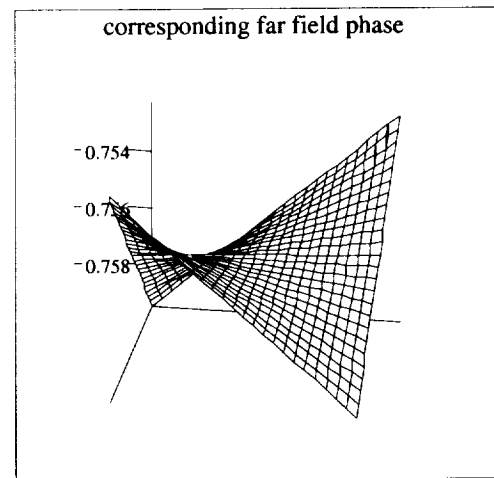
z13



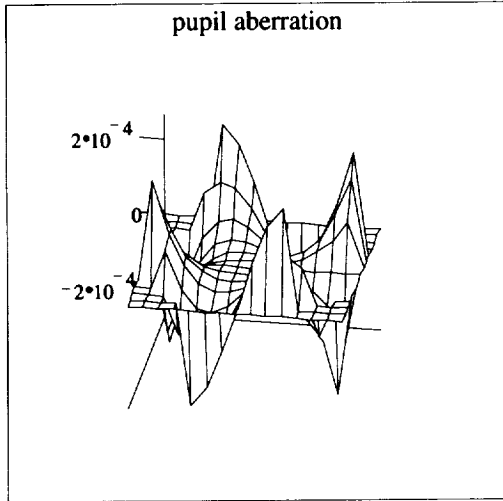
p13



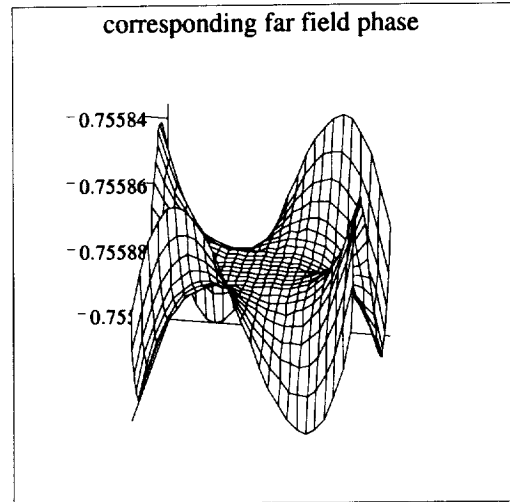
z14



p14



z15



p15

6. ANALYTIC EXPRESSIONS

Fitting Zernike polynomials to these far field phase variations (on a suitable circle) produces the following (to a suitable approximation) analytic expressions, where X and Y are the far field distances measured (in kilometers) from -2.64 to +2.64 kilometers. (When using the formula use $x=X/2.64$ and $y=Y/2.64$, the scaled to a unit circle coordinates.) The phase (in radians) variation, for a given $1/10 \lambda$ rms Zernike aberration on the 5 million kilometer sphere, is then given by the following formula along with the names of the exit pupil aberrations.

$$P4(x, y) := -1.34 \frac{1}{\sqrt{\pi}} + 6.21 \cdot 10^{-3} \cdot \left[-\sqrt{6} \cdot \frac{(-x^2 + y^2)}{\sqrt{\pi}} \right] \quad \text{Astigmatism 1}^{\text{st}} \text{ order } 0^\circ$$

$$P5(x, y) := -1.22 \frac{1}{\sqrt{\pi}} + 3.47 \cdot 10^{-3} \cdot \left[\sqrt{3} \cdot \frac{(-1 + 2 \cdot x^2 + 2 \cdot y^2)}{\sqrt{\pi}} \right] \quad \text{Defocus}$$

$$P6(x, y) := -1.34 \frac{1}{\sqrt{\pi}} + 7.04 \cdot 10^{-3} \cdot \left(2 \cdot \frac{\sqrt{6}}{\sqrt{\pi}} \cdot y \cdot x \right) \quad \text{Astigmatism 1}^{\text{st}} \text{ order } 0^\circ$$

$$P7(x, y) := -1.34 \frac{1}{\sqrt{\pi}} \quad \text{Trifoil } 0^\circ$$

$$P8(x, y) := -1.34 \frac{1}{\sqrt{\pi}} \quad \text{Coma X}$$

$$P9(x, y) := -1.34 \frac{1}{\sqrt{\pi}} \quad \text{Coma Y}$$

$$P10(x,y) := -1.34 \frac{1}{\sqrt{\pi}}$$

Trifoil 30°

$$P11(x,y) := -1.28 \frac{1}{\sqrt{\pi}} - 3.35 \cdot 10^{-4} \cdot \left[\sqrt{3} \cdot \frac{(-1 + 2 \cdot x^2 + 2 \cdot y^2)}{\sqrt{\pi}} \right]$$

Tetrafoil 0°

$$P12(x,y) := -1.34 \frac{1}{\sqrt{\pi}} - 2.1 \cdot 10^{-3} \cdot \left[-\sqrt{6} \cdot \frac{(-x^2 + y^2)}{\sqrt{\pi}} \right]$$

Astigmatism 2nd order 0°

$$P13(x,y) := -1.16 \frac{1}{\sqrt{\pi}} - 7.25 \cdot 10^{-4} \cdot \left[\sqrt{3} \cdot \frac{(-1 + 2 \cdot x^2 + 2 \cdot y^2)}{\sqrt{\pi}} \right]$$

Spherical

$$P14(x,y) := -1.34 \frac{1}{\sqrt{\pi}} - 1.23 \cdot 10^{-3} \cdot \left(2 \cdot \frac{\sqrt{6}}{\sqrt{\pi}} \cdot y \cdot x \right)$$

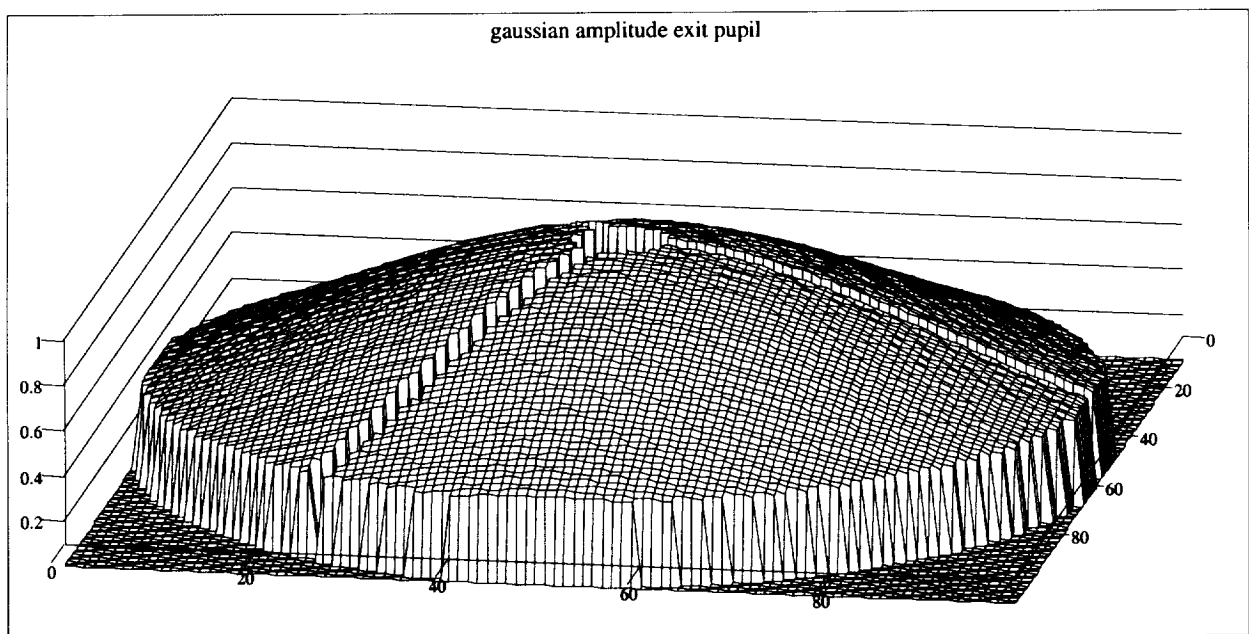
Astigmatism 2nd order 45°

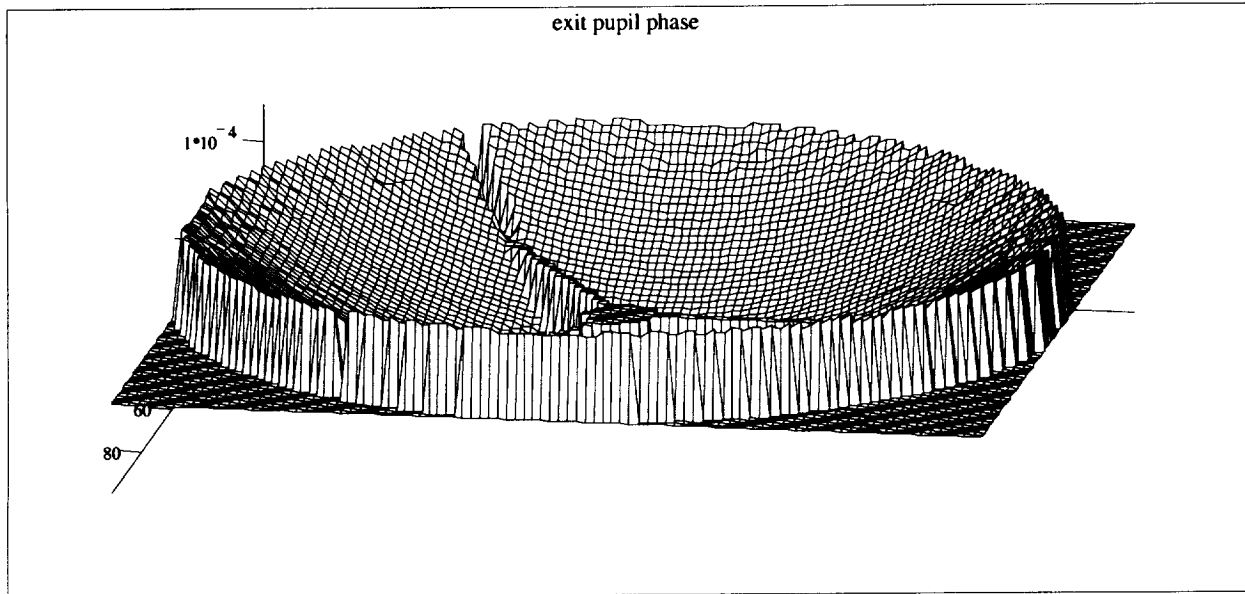
$$P15(x,y) := -1.34 \frac{1}{\sqrt{\pi}} - 1.19 \cdot 10^{-5} \cdot \left[-4 \cdot \sqrt{10} \cdot y \cdot x \cdot \frac{(-x^2 + y^2)}{\sqrt{\pi}} \right]$$

Tetrafoil 22.5°

7. GAUSSIAN BEAM, CENTRAL OBSCURATION, AND SUPPORTING STRUTS

The above results all assumed a uniformly illuminated exit pupil with no obscuration. This is a good starting point, however the real telescope may have obscurations and a Gaussian beam profile, in which case the exit pupil will appear as the following plots (with 1/10 λ defocus added for better visualization). The diameter of the pupil is 254 mm.

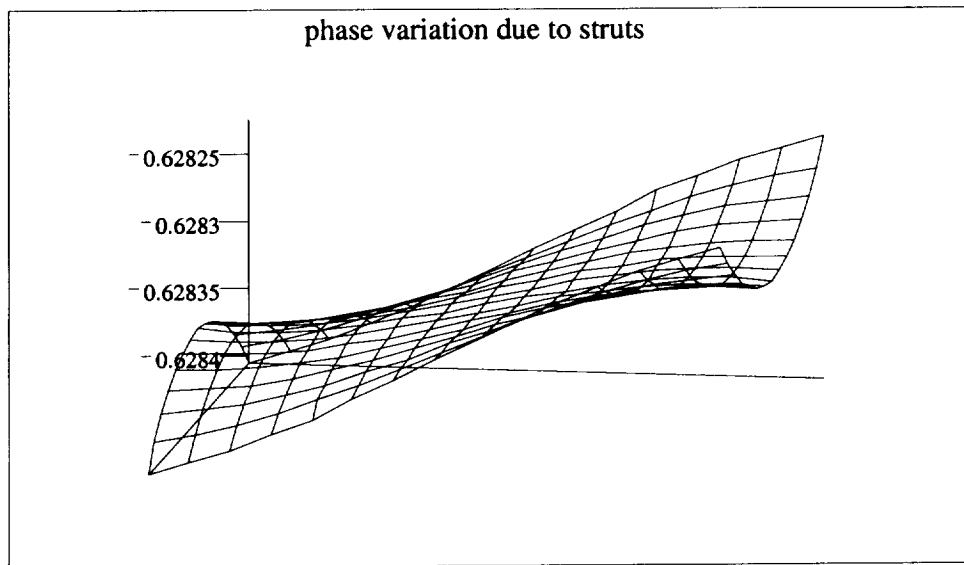




z4

The diameter of the central obscuration is 24 mm and the strut thickness is 10 mm.

For the unaberrated beam there is no phase variation on the 5 million kilometer sphere within the central peak as seen in the earlier plot. Now, adding only the obscurations and Gaussian beam profile but leaving the exit pupil phase "flat" (constant) does produce a variation in far field as is shown in the plot below.



P_z

The phase in this plot exhibits an asymmetry. This is due to the fact that there are only three struts with two of them on one side and only one on the other side (loosely speaking). This is what breaks the symmetry. The phase variation is very small, but present. As can be seen the predominant effect of the struts is to introduce tilt. An analytic expression for this curve (obtained by fitting Zernike polynomials within a appropriate circle) is

$$Phase(x,y) = \frac{-1.11}{\sqrt{\pi}} + 4.13 \cdot 10^{-5} \cdot \frac{2}{\sqrt{\pi}} \frac{y}{2.64} + 1.37 \cdot 10^{-5} \sqrt{\frac{8}{\pi}} \cdot y \cdot \left(\frac{3x^2 - y^2}{2.64^3} \right).$$

Where, as before, x and y are the far-field distances measured (in kilometers) from -2.64 to +2.64 kilometers (hence the factor in the denominator) and the phase variation, on the 5 million kilometer sphere, is in radians

8. CONCLUSION

As optical systems grow in size, and LISA is an example of a particularly long optical system, it is reassuring that analyzing them can still be performed with slightly modified existing analysis tools. All of the ray tracing was performed with QRAYPKS, a FORTRAN ray trace code written by the author. The code was modified to perform REAL*16 arithmetic, hence the leading "Q". A large portion of the analysis shown here only requires quadruple precision for the numerical sum that approximates the diffraction integral. It is possible to approach the problem analytically. However, "brute force" ray tracing has a distinct advantage in that the only question that arises is "did we fire enough rays?" For example, I would be hard pressed to generate the above "phase variation due to struts" plot using an analytical approach. But numerically it is straightforward. We have also shown some of the large scale (out to the second Airy dark ring) phase behavior and some of the phase behaviour right around the central peak. All of the plots and analysis not requiring quad precision were performed using MATHCAD™.

ACKNOWLEDGMENTS

This work was performed at JILA, a joint institute of the National Institute of Standards and Technology and the University of Colorado at Boulder and supported by a Goddard Space Flight Center's Fellowship.

REFERENCES

1. *Laser Interferometer Space Antenna for the detection and observation of gravitational waves*, Pre-Phase A Report, Second Edition, July 1998.
2. M. Born and E. Wolf, *Principles of Optics*, Pergamon Press, 1980.
3. B.R.A. Nijboer, *Physica*, 10 (1943), 679; *ibid.*, 13 (1947), 605.